Spectral Sensitization of TiO_2 Substrates by Monolayers of Porphyrin Heterodimers

Rob B. M. Koehorst,*,† Gerrit K. Boschloo,‡,§ Tom J. Savenije,†,⊥ Albert Goossens,‡ and Tjeerd J. Schaafsma†

Laboratory of Molecular Physics, Department of Biomolecular Sciences, Wageningen University, Dreijenlaan 3, 6703 HA Wageningen, The Netherlands, and Laboratory for Inorganic Chemistry, Faculty of Applied Sciences, Delft University of Technology, Julianalaan 136, 2628 BL Delft, The Netherlands.

Received: November 15, 1999

Photoelectrochemical cells have been constructed by depositing monolayers of oriented covalently linked zinc/free base porphyrin heterodimers onto ∼30 nm nonporous layers of TiO_2 on ITO, deposited by metal−organic chemical vapor deposition (MO-CVD), and onto ∼100 nm porous, nanostructured TiO_2 layers, spin-coated from a suspension of P25 (Degussa) on ITO. Fluorescence quenching of the dyes on both types of TiO_2 substrates is compared with that of dilute solutions of the dyes and with that of dye-coated, porous ZrO_2 (Degussa) substrates. By functionalizing one of the porphyrin dimer components with carboxylic substituents, which bind to the TiO_2 or ZrO_2 substrate surface, either the zinc porphyrin (ZnP) or the free base porphyrin (H_2P) component of the dimer can be made to be in direct contact with the substrate. These dimer−substrate arrangements are denoted ZnP−H_2P- -TiO_2 (dimer **1**) and H_2P−ZnP- -TiO_2 (dimer **2**), respectively, where "- -" denotes binding of the carboxyl-substituted porphyrin in the heterodimer to the substrate surface. In solution as well as deposited on ZrO_2, in contact with the solvent without a redox couple, both types of dimers show efficient internal ZnP to H_2P energy transfer. Deposited on TiO_2, in the presence of the solvent, monolayers of both types of dimers show less efficient energy transfer than the dimers on ZrO_2. For a ZnP−H_2P- -TiO_2 electrochemical cell the photocurrent action spectrum reproduces the absorption spectrum, i.e., contains contributions of both the ZnP and H_2P moieties. By contrast, for H_2P−ZnP- -TiO_2 cells mainly the ZnP dimer component contributes to the photocurrent, demonstrating that in H_2P−ZnP- -TiO_2 cells electron transfer from the ZnP into the TiO_2 substrate is faster than energy transfer to the adjacent free base porphyrin. The photocurrent action spectrum of the ZnP−H_2P- -TiO_2 cell also demonstrates that energy transfer in monolayers of this dimer results in sensitization of the semiconductor substrate, since the spectral response of a cell is enhanced with respect to that of a cell with a monolayer of a monomeric sensitizer. These results are relevant for the construction of a solar cell containing a supramolecular, light-collecting antenna.

1. Introduction

Metal oxide semiconductors have been spectrally sensitized by making use of (metallo-) organic dyes such as Ru-bipyridyl (Ru(bipy)) complexes,[1−3] chlorophyll analogues,[4−10] porphyrins,[11−15] and phthalocyanines.[16−20] Recently, cosensitization by mixtures of different porphyrins and mixtures of porphyrins and phthalocyanines has been reported.[21,22] In sandwich-type cells, porphyrins have been applied as (ordered) films between metal and/or indium/tin oxide (ITO) electrodes.[23−29]

For dye-sensitized photoelectrochemical solar cells, Grätzel et al. sensitized nanostructured TiO_2 using various Ru(bipy) complexes[1,2] achieving energy conversion efficiencies of ∼12% in diffuse daylight[1] and 10% for AM 1.5 simulated sunlight.[2] Recently, also solid state cells have been described, using various pigments adsorbed on n-TiO_2[30−35] or n-SnO_2.[36,37] Solid state dye-sensitized cells, using an (ultra)thin porphyrin layer on flat nonporous TiO_2, have been the subject of recent studies.[12] Since in this type of cells the sensitizer layer absorbs only a fraction of the incident light, it is necessary to increase the light absorption by using a ∼100 nm thick dye layer, which should be able to transport the excitation energy to the photoactive porphyrin/semiconductor interface, and thus acts as an antenna.

Photovoltaic cells have also been constructed by using two layers of different dyes with electron-donating and -accepting properties, respectively, resulting in heterojunction cells showing unidirectional photoinduced electron transfer at the interface of the two dye layers.[37−46]

Mixed layers of porphyrins can form heterodimers via functional groups at the meso-aryl position. Sandwich cells containing these mixed layers show higher conversion efficiencies than the same cells containing a single type of porphyrin.[27,44] Specific interaction between the different porphyrins in heterodimers appears to be necessary to enhance the conversion efficiency, since no photocurrent increase was observed by replacing a spin-coated layer of porphyrin monomers by a spin-coated layer of covalently bound, cofacial, diporphyrins in a sandwich cell.[23]

A solid state cell making use of resonance energy transfer between two layers of different dyes was reported earlier,[37] and a device having a dye with antenna function, using Ru(bipy) dyes, has been proposed by Bignozzi et al.[47] Photosensitization

* Author to whom correspondence should be addressed. E-mail: Rob.Koehorst@FOTO.MF.WAU.NL.

† Wageningen University.

‡ Delft University of Technology.

§ Present address: Department of Physical Chemistry, Uppsala University, P.O. Box 532, S-751 21 Uppsala, Sweden.

⊥ Present address: Radiation Chemistry Department, IRI, Delft University of Technology, Mekelweg 15, 2629 JB, Delft, The Netherlands.

10.1021/jp994044+ CCC: $19.00
Published on Web 02/18/2000

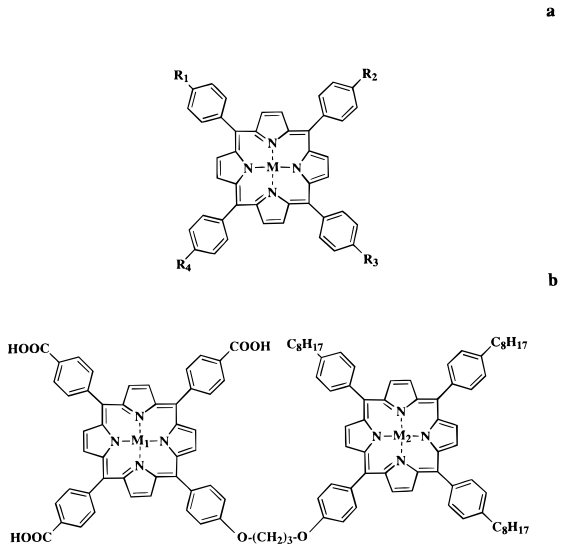

Figure 1. Structures of (a) porphyrin monomers $ZnPC_4$ (M = Zn, R1 = R2 = R3 = R4 = COOH); $ZnPC_3$ (M = Zn, R1 = R2 = R3 = COOH, R4 = H); $ZnPC_2$ (M = Zn, R1 = R2 = COOH, R3 = R4 = H); $ZnPC_1$ (M = Zn, R1 = COOH, R2 = R3 = R4 = H); and H_2PC_4 (M = 2H, R1 = R2 = R3 = R4 = COOH); and (b) dimer **1** (M1 = 2H, M2 = Zn), and dimer **2** (M1 = Zn, M2 = 2H).

of a solid state cell employing monolayers of heterodimers asymmetrically chemisorbed onto colloidal TiO_2 has recently been reported.[48] However, only photophysical data of the dye were presented. In this paper, we report spectral sensitization of TiO_2 by monolayers of porphyrin heterodimers, containing a light-collecting antenna function. For that purpose, one of the dimer components is brought into direct contact with the TiO_2 substrate by selectively functionalizing this component with up to three carboxylic substituents. The other dimer component has three *p*-octylphenyl substituents and is covalently bound to the first one through a propylene−diether bridge (Figure 1b). This approach is different from the above-mentioned cosensitization[21,22] of a semiconductor, in view of the spatial arrangement of the porphyrin moieties in the covalently linked dimers in the present study.

We have investigated energy and electron transfer processes in covalently bound porphyrin heterodimers bound to the TiO_2 substrate**.** For one of the dimers one of its components acts as an antenna and the other as energy trap and electron donor for TiO_2. Either one of the dimer components, i.e., the one in direct contact with TiO_2 (as for dimer **2**), or the one on top of it (as for dimer **1**) may act as an energy donor for the other, noting that energy transfer only proceeds from the zinc porphyrin to the free base.[49,50]

This paper reports the photophysical and photoelectrochemical properties of sensitized porphyrin/TiO_2 assemblies, using various porphyrin monomers and heterodimers. As a reference we used porphyrin monomers and heterodimers on ZrO_2 substrates with very similar binding properties, but without photoinduced electron transfer from the porphyrin to the substrate. Energy transfer competitive and consecutive, respectively, with electron transfer is observed in the dimer/TiO_2 assemblies, demonstrating the principle of a light-collecting antenna feeding a photoactive electron donor at a semiconductor interface.

2. Experimental Section

Porphyrins functionalized with carboxylic substituents can be bound to a TiO_2 surface, as reported for the reference compound zinc tetrakis(4-carboxyphenyl)porphyrin, $ZnPC_4$ (Figure 1a).[11] $ZnPC_4$ and its free base analogue H_2PC_4 (Aldrich) were purchased or obtained by hydrolyzing the ester groups of the symmetrical tetrakis(4-carbomethoxy)phenylporphyrin precursor from a mixed aldehyde synthesis. Since the electron injection efficiency may depend on the number of carboxyl groups and on the resulting orientation of the porphyrin plane with respect to the substrate surface,[51] we included also porphyrins with one to three carboxyphenyl substituents. Zinc complexes of 5-mono(4-carboxy)phenylporphyrin ($ZnPC_1$), 5,10-di(4-carboxy)phenylporphyrin ($ZnPC_2$), and 5,10,15-tri(4-carboxy)phenylporphyrin ($ZnPC_3$) were obtained by hydrolyzing the methyl ester derivatives after zinc was inserted into the free base by standard methods.[52] The methyl esters were synthesized by the mixed aldehyde procedure.[53]

The dimer precursors 5-mono(4-hydroxyphenyl)-10,15,20-tris(4-carbomethoxyphenyl)porphyrin and 5-mono(4-hydroxyphenyl)-10,15,20-tris(4-octylphenyl)porphyrin were synthesized by the mixed aldehyde method. Both porphyrins were covalently linked following published methods,[54] after complexing one of them with zinc followed by hydrolysis of the ester groups to obtain the desired carboxy dimers $H_2P(COOH)_3-ZnP(C_8H_{17})_3$ (**1**) and $ZnP(COOH)_3-H_2P(C_8H_{17})_3$ (**2**) (Figure 1b). The carboxylic ester derivatives were chromatographically purified over silica gel (Merck) with analytical grade CH_2Cl_2 (Merck) with increasing relative amounts of methanol as the number of esther-groups of the eluting porphyrin increases. The porphyrins are estimated to be >99% pure as shown by thin-layer chromatography and absorption, fluorescence, and ^1H NMR spectroscopies.

ITO-covered glass slides (Glastron; 30 Ω/□) were coated with TiO_2 by evaporation, using Ti(IV) isopropoxide and oxygen as the precursors, yielding amorphous, nonporous layers of 30 nm thickness. The nanostructured TiO_2 layers of ∼100 nm thickness were obtained by spin-coating a stabilized terpinol-based P25 (Degussa) screenprint paste,[55] diluted with *n*-butanol (1:4 w/w), onto ITO. The substrates thus obtained were heated for 30 min to 100 °C and then sintered for 15 min at 450 °C. The same procedure was followed to prepare ∼100 nm thick, nanostructured ZrO_2 layers, using a screenprint ZrO_2 paste (E8, Degussa).

The porphyrin derivatives were adsorbed at TiO_2 or ZrO_2 substrates from 10^{-5} to 10^{-4} M ethanol solutions or 1:1 ethanol/toluene mixtures immediately after heating the substrates to 100 °C for 10 min to remove adsorbed moisture. The coated substrates were rinsed with ethanol or a 1:1 ethanol/toluene mixture, dried with a nitrogen jet, and additionally dried in air at 100 °C for 10 min.

Absorption spectra of porphyrin solutions were recorded using a Cary 5E spectrometer. For virgin substrates and substrates with adsorbed porphyrin layers the same Cary 5E spectrometer was used equipped with a 150 mm o.d. integrating sphere (DRA-CA-50, Labsphere) to correct for scattering. Solid samples were positioned in the center of the sphere at an angle of 10° between the normal and the incident light beam to avoid specularly reflected light from leaving the sphere by the entrance port.

Fluorescence spectra of solutions were recorded using a Perkin-Elmer LS5 fluorimeter, whereas for solid samples placed in a cuvette holding propylene carbonate as a solvent a SPEX Fluorolog 3-22 fluorimeter was used using front face fluorescence detection. The solutions were excited at the wavelength (550 nm) of the strongest zinc porphyrin Q absorption band whereas samples with adsorbed monolayers were excited at the 430 nm Soret absorption maximum using a 530 nm cutoff filter and monochromator slit widths with 5 nm nominal band-pass both in excitation and emission.

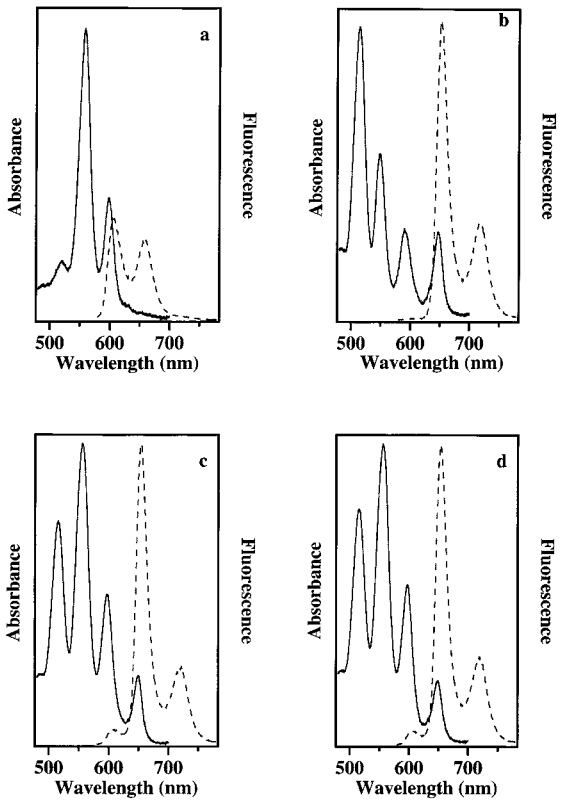

Figure 2. Q-band absorption (solid lines) and fluorescence spectra (broken lines) of ethanol solutions of (a) $ZnPC_4$, (b) H_2PC_4, (c) dimer **1,** and (d) dimer **2**. Note that vertical scales are different except for the monomer fluorescence spectra (a, b) in which relative intensities are shown for equimolar solutions. (For experimental details see text.)

Fluorescence excitation spectra were recorded by detection at the maximum (725 nm) of the free base $Q_{0,1}$ fluorescence and varying the excitation wavelength from 470 to 670 nm. Fluorescence excitation spectra were corrected for the lamp output up to 600 nm, limited by the Fluorolog 3-22 specifications.

For photoelectrochemical measurements we used an electrochemical cell containing 0.05 M I_2/0.5 M KI in 1:1 v/v propylene−ethylene carbonate sandwiched between the porphyrin-coated TiO_2/ITO electrode and a Pt sputtered ITO substrate as a counter electrode. The electrodes were separated by a 0.2 mm Teflon spacer. An area of 0.5 cm^2 of the cell was illuminated with light from a 150 W xenon lamp (Spectral Energy) which passed through a monochromator GM 252 (Spectral Energy) with 20 nm nominal band-pass and a 380 nm cutoff filter to prevent absorption of UV light by the TiO_2 substrate. The light intensity at 430 nm was ∼1 mW/cm^2, measured with a Thermopile CA1 (Kipp & Zonen, Delft, The Netherlands). Irradiation took place through the TiO_2 electrode, and photocurrents were recorded under short-circuit conditions.

3. Results and Discussion

3.1. Optical Spectra of Porphyrins in Solution. Figure 2a−d shows absorption and fluorescence spectra of the monomers and heterodimers in ethanol. The dimer fluorescence spectra (Figure 2c,d) both show 650 and 725 nm fluorescence bands very similar to the fluorescence spectrum of the free base monomer (H_2PC_4) presented in Figure 2b. The fluorescence band around 600 nm of the ZnP moiety is quenched for about ∼80−90% in the heterodimers. The excitation spectrum of the 725 nm dimer fluorescence of the H_2P moiety (not shown) is very similar to the absorption spectrum for both dimers **1** and **2**, indicating ZnP to H_2P energy transfer. By contrast, H_2P to ZnP energy transfer evidently does not occur because the excitation spectrum of the 600 nm dimer fluorescence of ZnP shows only ZnP absorption bands (not shown). This agrees with earlier results for other zinc-/free base tetra-phenylporphyrin heterodimers.[50]

3.2. Optical Spectra of Porphyrins on TiO_2/ZrO_2. *3.2.1. Absorption Spectra.* For various porphyrin monomers $ZnPC_{1-4}$ and H_2PC_4 (Figure 1a) adsorbed on nonporous TiO_2−ITO substrates, the intensities of the transmitted and scattered light on the average add up to ∼91% at 430 nm, amounting to an absorbance of 0.04 corresponding to monolayer coverage.[49] An intensity ratio of approximately 0.5 was found for the Soret band of monolayers of the monomers and the dimers. From this result, adsorption of the amphiphilic heterodimers onto nonporous TiO_2 from a 1:1 v/v ethanol/toluene solution, followed by rinsing with the same solvent mixture, is also expected to result in monolayer coverage. Because P25 and ZrO_2 layers cannot be reproduced with the same thickness and morphology by spin-coating, yielding differences in intensities of reflected light, the maximum absorbance of the Soret band has a spread of 20%.

The absorption spectra in the Q-band region of monolayers of the monomers $ZnPC_4$ and H_2PC_4, and of the dimers **1** and **2** on P25 TiO_2 are presented in Figure 3, a and c. The Soret bands are slightly red-shifted and broadened with respect to the solution spectra and do not show separate ZnP and H_2P contributions. Absorption spectra of porphyrin monomers with different number of carboxylic groups on TiO_2 are very similar to those of $ZnPC_4$ and H_2PC_4. Spectra of monolayers on nonporous TiO_2 and ZrO_2 are identical to those on porous TiO_2, except for the intensity.

3.2.2. Fluorescence Spectra. Fluorescence spectra of the dye-coated P25 TiO_2 and ZrO_2 substrates are essentially the same as those recorded from solutions of the corresponding dye. For clarity reasons, only spectra of dye-coated P25 TiO_2 are therefore presented (Figure 3b,d). Figure 3b shows fluorescence spectra of monolayers of the porphyrins $ZnPC_4$ and H_2PC_4 on porous TiO_2. For both compounds, no spectral differences were observed for a different number of carboxylic side groups.

Quantitative comparison of fluorescence yields of monolayers of monomers and heterodimers is difficult because of variations in the structure of the surface and in the thickness of the metaloxide layers. However, *electron transfer* competitive with *energy transfer* is clearly demonstrated by comparing excitation spectra of the 725 nm H_2P fluorescence of dimer/TiO_2 and dimer/ZrO_2 samples. Fluorescence excitation spectra of monolayers of dimer **1** (Figure 3e) and of dimer **2** (Figure 3f) on ZrO_2 substrates are very similar and closely resemble the solution spectra. Note, however, that the fluorescence excitation spectra of monolayers of dimer **1** (Figure 3e) and of dimer **2** (Figure 3f) on P25 TiO_2 both show a decreased contribution around 555 and 600 nm excitation with respect to those of the corresponding dimers on ZrO_2.

For all monomeric dyes adsorbed on the inert ZrO_2, after excitation no other processes take place than those in dilute solutions, except for lateral *energy transfer* between identical dye molecules. However, when these dyes are adsorbed on TiO_2 *electron transfer* from the excited TiO_2-bound porphyrin is expected to compete with these processes. Similarly, excitation of the TiO_2-bound porphyrin moiety of the heterodimers also results in electron transfer to the substrate. For dimer **2** electron transfer from the excited ZnP moiety (ZnP*) is expected to compete with energy transfer to the H_2P moiety (Figure 4b).

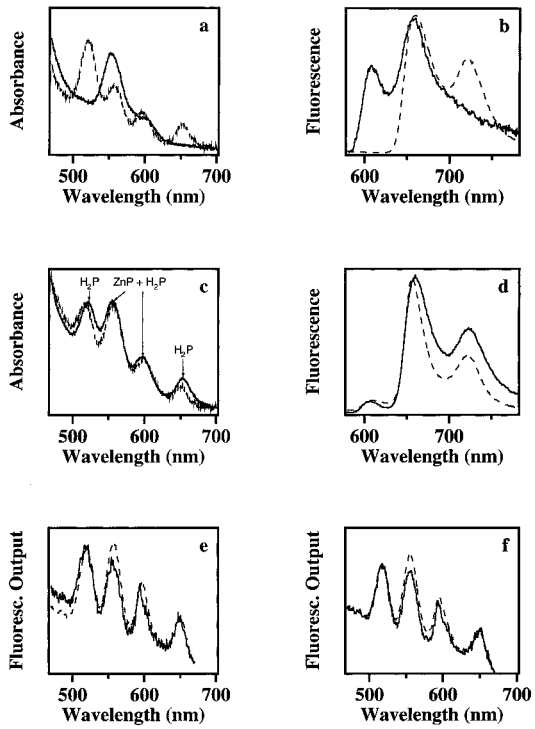

Figure 3. (a, c) Q-band absorption spectra; (b, d) fluorescence spectra of monolayers of $ZnPC_4$ and H_2PC_4 (solid and broken lines, respectively, in a and b), of dimer **1** (solid lines in c and d) and of dimer **2** (broken lines in c and d) on porous P25 TiO_2. Parts a−d have different vertical axes for clarity reasons. (e) Q-band fluorescence excitation spectra detected at 725 nm for P25 TiO_2 (solid lines) and ZrO_2 (broken lines) coated with dimer **1**; (f) coated with dimer **2**. The spectra in (e) and (f) are normalized at the free base Q-band located around 525 nm. (For experimental details see text.)

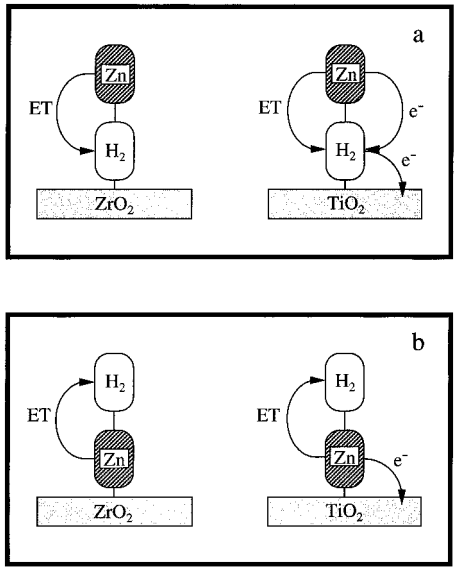

Figure 4. Scheme for energy (ET) and electron transfer (e^-) in (a) oriented monolayers of dimer **1** and (b) dimer **2** on ZrO_2 (left) and TiO_2 (right) following selective excitation of the ZnP moiety.

This accounts for the observed decrease around 555 and 600 nm in the excitation spectrum of the fluorescence of dimer **2** on P25 TiO_2 with respect to that of dimer **2** on ZrO_2 (Figure 3f) . The maxima of the two main Q-bands of the ZnP absorption spectrum coincide with the above-mentioned wavelengths. Dimer **1** has also a decreased ZnP contribution to the fluorescence excitation spectrum of this dimer on P25 TiO_2 with respect to that of dimer **1** on ZrO_2 (Figure 3e). Because electron transfer from the excited H_2P moiety (H_2P^*) into TiO_2 only takes place after energy transfer from ZnP* to the H_2P (Figure 4a), it is expected that the ZnP contribution to the fluorescence excitation spectrum is similar to that of dimer **1** on ZrO_2. To account for the differences in photophysical behavior of dimer **1** on both substrates we have to consider intramolecular electron transfer between the ZnP and the H_2P moiety in the heterodimers.

Possible electron transfer reactions in the various dimer/substrate arrangements are given by the equations:

$$H_2P^- - ZnP^+ \text{- -}TiO_2 \xleftarrow{(2)} H_2P - ZnP^* \text{- -}TiO_2 \xrightarrow{(1)} H_2P - ZnP^+ \text{- -}TiO_2^-$$

$$H_2P^- - ZnP^+ \text{- -}ZrO_2 \xleftarrow{(2')} H_2P - ZnP^* \text{- -}ZrO_2 \dashrightarrow H_2P - ZnP^+ \text{- -}ZrO_2^-$$

$$ZnP^* - H_2P \text{- -}TiO_2 \xrightarrow{(3)} ZnP^+ - H_2P^- \text{- -}TiO_2 \xrightarrow{(4)} ZnP^+ - H_2P \text{- -}TiO_2^-$$

$$ZnP^* - H_2P \text{- -}ZrO_2 \xrightarrow{(3')} ZnP^+ - H_2P^- \text{- -}ZrO_2 \dashrightarrow ZnP^+ - H_2P \text{- -}ZrO_2^-$$

Intramolecular electron transfer from ZnP to H_2P in dimer **2** on TiO_2 (2) competes with electron injection from ZnP* into the TiO_2 (1). Both processes result in a decrease of the steady state concentration of ZnP*, from which H_2P^* is populated, compared to a situation where electron transfer into the substrate is forbidden, as for the ZrO_2 substrate. On the other hand, intramolecular electron transfer from ZnP* to H_2P in dimer **1** (3, 3′) can subsequently be followed by electron transfer from reduced H_2P for TiO_2 as the substrate (4), but not for ZrO_2.

Effectively, reaction 4 following the intramolecular electron transfer from ZnP* to H_2P in $ZnP-H_2P$- -TiO_2 (3) results in a lower steady state concentration of ZnP*, from which H_2P^* is populated by energy transfer, than results from the intramolecular electron transfer from ZnP* to H_2P in $ZnP-H_2P$- -ZrO_2 (3′).

For dimer **1** as well as dimer **2** in ethanol solution the fluorescence of H_2P is not quenched with respect to that of the free base monomer H_2PC_4. In addition, excitation spectra of the H_2P fluorescence in the heterodimers reveal that quenching of the ZnP fluorescence in the heterodimers in solution results from energy transfer rather than intramolecular electron transfer. Referring to the above-mentioned experimental results, electron transfer is even more unlikely in the dimers on TiO_2 or ZrO_2 because of destabilization of the intramolecular charge separated $ZnP^+-H_2P^-$ state in the adsorbed monolayer, due to the loss of solvent reorientation energy.[56] This has been demonstrated by comparing fluorescence quenching in porphyrin donor−acceptor heterodimers in liquid solution and a sucrose glass.[57] Upon freezing to a solid glass, fluorescence quenching was only observed for heterodimers for which the energy of the charge separated D^+-A^- state is so far below the first excited singlet state of either porphyrin that destabilization of the D^+-A^- state upon freezing the solution does not shift this state above the close-lying S_1 states of donor and acceptor. From these experimental results the solvent reorientation energy can be estimated as 0.8−0.9 eV, in agreement with previous findings for other donor−acceptor compounds.[58] In dimer **2** on TiO_2 (H_2P-ZnP- -TiO_2), intradimer electron transfer from ZnP to H_2P^* or from ZnP* to H_2P is even more unlikely because the

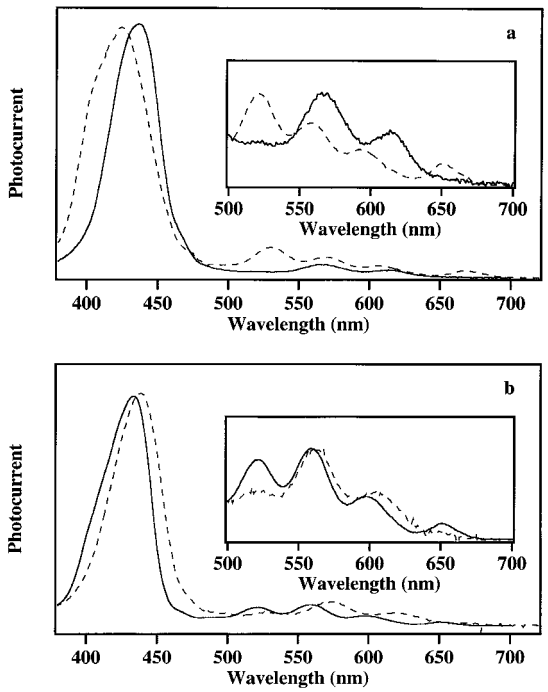

Figure 5. Photocurrent action spectra of photoelectrochemical cells of type ITO/TiO_2/dye/(I_2/I_3^-)/Pt for monolayers of $ZnPC_4$ (a, solid line), H_2PC_4 (a, broken line), dimer **1** (b, solid line), and dimer **2** (b, broken line) normalized at the maximum of the Soret band. The insets show the Q-bands of the same spectra at a different scale and normalized at the Q-bands with highest intensity (for experimental details see text).

TiO_2 (electron withdrawing) will affect the redox properties of the bound ZnP. In the reaction scheme given above, the rate constants for reaction 2 and 2′ are small compared to that for reaction 1. However, in dimer **1** on TiO_2 (ZnP−H_2P- -TiO_2) the effect of binding to TiO_2 on the redox properties of H_2P favors intradimer electron transfer from ZnP* to H_2P followed by electron transfer from the reduced primary acceptor (H_2P^-) to the TiO_2 substrate. Thus, the rate constant for reaction 3 exceeds that for reaction 3′.

The various photophysical processes following excitation of the ZnP moiety in the two substrate-bound heterodimers are schematically presented in Figure 4 for dimer **1** (Figure 4a) and for dimer **2** (Figure 4b), considering solely intradimer electron transfer in ZnP−H_2P- -TiO_2 because of the favorable arrangement of primary electron donor ZnP* and primary electron acceptor H_2P with respect to the final electron acceptor TiO_2.

To corroborate the above-mentioned arguments about the electron transfer efficiencies of both dimer components and energy transfer consecutive and competitive, respectively, with electron transfer in these dimers, complete cells using porphyrin-coated TiO_2 were illuminated resulting in the photocurrent action spectra, described below.

3.3. Photocurrent Action Spectra. For each of the porphyrin monomers as well as for dimer **1**, both on nonporous and porous TiO_2, the photocurrent action spectra agree with the absorption spectra (cf. Figures 3 and 5). By contrast, this is not found for dimer **2**. Note that in Figure 5b the photocurrent action spectrum in the 500−700 nm wavelength range of a monolayer of dimer **1** contains contri-butions of both dimer components, whereas that of a monolayer of dimer **2** shows mainly ZnP contributions. Because the results for dye-sensitized nonporous TiO_2 are similar to those for porous TiO_2 only spectra for the latter are presented.

The photocurrent action spectra as well as the absorption and fluorescence spectra of the various porphyrin monomers are

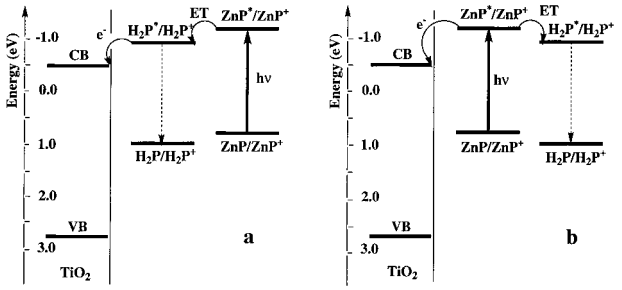

Figure 6. Energy levels (eV vs NHE) of the semiconductor valence (VB) and conduction bands (CB), and of the oxidation potential in the ground (P/P^+) and excited state (P^*/P^+) of both porphyrins in (a) dimer **1** and (b) dimer **2**.

unaffected by varying the number of carboxyphenyl side groups. This is a clear indication that only one carboxylphenyl group can be bound to the TiO_2 substrate, probably for steric reasons, resulting in a similar orientation of the porphyrin macrocycle with respect to the surface for each of the different monomers. Assuming a similar orientation and distance of each of the monomers with respect to the surface from a single porphyrin−TiO_2 bond, a through-space electron transfer mechanism is most likely to explain the observed photocurrent action spectra.

The photocurrent action spectra of monolayers of dimer **1** and of dimer **2** are expected to be different since the excitation transfer from the ZnP to the H_2P moiety is unidirectional. Figure 6a,b depicts the relevant energetics for the photophysical processes of dimer **1** and dimer **2**, respectively. In dimer **1** excitation of either the ZnP or the H_2P moiety results in excited H_2P close to the TiO_2 surface which therefore can easily inject an electron into the TiO_2 substrate. Intramolecular electron transfer also results in photocurrent from dimer **1** because of the earlier mentioned secondary electron transfer step but is omitted in Figure 6 for reasons of clarity. When energy donor and acceptor are in reverse order with respect to the TiO_2 substrate, as in dimer **2** (Figure 6b), ZnP* to H_2P energy transfer competes with electron injection into the TiO_2 substrate. If the excited state is localized on the H_2P part in dimer **2** (by direct excitation or energy transfer from the ZnP) electron injection from H_2P* into TiO_2 is less likely to occur because of its larger distance to the TiO_2, in accordance with experiment (Figure 5b).

Noting that (i) only excitation of the TiO_2-linked ZnP moiety in dimer **2** produces a photocurrent and (ii) excitation of both the ZnP and the H_2P moiety in dimer **1** results in a photocurrent, the interrelation between fluorescence quenching and electron transfer, both intramolecular and at the dye-TiO_2 interface, are confirmed by the fluorescence and photocurrent results. The intimate relation between fluorescence quenching vs an applied bias voltage and photocarrier generation in a chlorophyll-*a*-coated nanocrystalline SnO_2 film was convincingly demonstrated by Kamat et al.[6]

Although the maximum photocurrents exhibit some spread, the photocurrents for dimer **1** and **2** are practically the same and somewhat larger than that for the $ZnPC_4$ and H_2PC_4 monomers. This implies that the rate constant for ZnP* to TiO_2 electron transfer in dimer **2** must at least be comparable to that for energy transfer to the H_2P moiety, in accordance with the above-mentioned fluorescence results. For dimer **1** and **2** the maximum current upon excitation with ∼1 mW/cm^2 incident light at the Soret absorption maximum at 430 nm is 10(±1) mA/cm^2, corresponding to an IPCE value of ∼3% and 3(±0.3) mA/cm^2 for the $ZnPC_4$ and H_2PC_4 monomers, yielding an IPCE value of ∼1%, and demonstrating the favorable effect of a light-

collecting antenna on the cell performance. In view of the fluorescence results the relative intensities of the observed photocurrents from dimer- and monomer-sensitized TiO_2 are not completely clear, however. Probably, attaching an antenna molecule to the surface-linked sensitizer molecule has an (as yet not completely understood) effect on the rate constant for charge recombination between the electron and sensitizer cation (e.g., hole transport in dimer **1**). Also, the rate constant for intersystem crossing to the triplet state for the excited surface-bound sensitizer may be enhanced by I_2. This is expected to affect the photocurrent yield because the triplet state is substantially lower in energy than the excited singlet state. The effect of I_2 may be decreased by the presence of the attached antenna moiety, especially with bulky C_8H_{17} groups partly covering the underlying surface-bound sensitizer molecule.

Our results show that at the surface of the relatively flat, nonporous TiO_2 layer and within the voids of the porous layers of nanosized TiO_2 particles the heterodimers are organized with respect to the surface in such a way that the non-carboxy-substituted dimer components are at relatively large distance from the substrate. As a final remark, we note that the finding that the H_2P moiety in dimer **2** does not contribute to the photocurrent can also be ascribed to the absence of a carboxyl link to the TiO_2 substrate. However, sensitization of TiO_2 with a spin-coated layer of free base tetra(4-(*n*-octyl)phenyl)porphyrin, lacking carboxyl groups, has been reported[59] and has also been found for a spin-coated layer of zinc tetra(4-(*n*-octyl)-phenyl)porphyrin.[60]

Summarizing our results, energy transfer and electron transfer in monolayers of dimer **1** on TiO_2 are shown to be *consecutive* whereas in monolayers of dimer **2** both processes are *competitive*.

4. Conclusions

The results of our investigations reveal that for a TiO_2 electrode covered with a monolayer of an asymmetrically functionalized porphyrin heterodimer, absorption by the antenna molecule in the dimer contributes to the photocurrent through transfer of excitation energy to the surface-bonded moiety, demonstrating supersensitization of a wide band gap semiconductor using a light-harvesting antenna. Introducing octyl chains at the para position of all four meso phenyl groups as in zinc tetra(4-(*n*-octyl)phenyl)porphyrin (ZnTOPP) results in semiordered layers after spin-coating from toluene solution.[45,60] When a ZnP−H_2P- -TiO_2 cell containing ZnP substituted with octyl chains at the para position of the three meso phenyl groups is covered by a spin-coated film of ZnTOPP, the ZnP dimer component may participate in the stacking of the ZnTOPP molecules. For these extended assemblies, excitons created in the bulk ZnTOPP layer can be trapped at the ZnP component of the heterodimer and subsequently be transferred to the TiO_2-bound H_2P component of the dimer as is demonstrated in this paper for the heterodimer monolayers. The trapped exciton can subsequently be dissociated into an electron and a hole at the H_2P/TiO_2 interface, resulting in a photocurrent as is also demonstrated in this work. Supersensitization by an organized molecular antenna on top of a charge separating dye/TiO_2 interface is currently further investigated. A molecular antenna layer of ~100 nm thickness should provide nearly 100% absorption of the solar spectrum.

Combining an efficiently charge injecting layer with a supersensitizing, charge-transporting molecular antenna represents a promising approach to increase the photocurrent yield of organic solar cells, provided the exciton path length of the antenna is not much smaller than its absorption length.

Acknowledgment. We are indebted to Dr. M. M. Wienk at The Netherlands Energy Research Foundation (ECN) for a generous gift of the porous TiO_2 and ZrO_2 substrates. This work was partly financed by The Netherlands Agency for Energy and Environment (NOVEM) under contract no. 146.100-024.4.

References and Notes

(1) O'Regan, B.; Grätzel, M. *Nature* **1991**, *353*, 737.
(2) Nazeeruddin, M.; Kay, A.; Rodicio, I.; Humphry-Baker, R.; Müller, E.; Liska, P.; Vlachapoulos, N.; Grätzel, M. *J. Am. Chem. Soc.* **1993**, *115*, 6382.
(3) Fessenden, R. W.; Kamat, P. V. *J. Phys. Chem.* **1995**, *99*, 12902.
(4) Kamat, P. V.; Chauvet, J. P.; Fessenden, R. W. *J. Phys. Chem.* **1986**, *90*, 1389.
(5) Hotchandani, S.; Kamat, P. V. *Chem. Phys. Lett.* **1992**, *191*, 320.
(6) Yang, Y.; Zhou, R.; Han, Y.; Jiang, Y. *J. Photochem. Photobiol., A* **1993**, *76*, 111.
(7) Kay, A.; Grätzel, M. *J. Phys. Chem.* **1993**, *97*, 6272.
(8) Kay, A.; Humphry-Baker, R.; Grätzel, M. *J. Phys. Chem.* **1994**, *98*, 952.
(9) Bedja, I.; Hotchandani, S.; Carpentier, R.; Fessenden, R. W.; Kamat, P. V *J. Appl. Phys.* **1994**, *75*, 5444.
(10) Bedja, I.; Kamat, P. V.; Hotchandani, S. *J. Appl. Phys.* **1996**, *80*, 4637.
(11) Kalyanasundaram, K.; Vlachopoulos, N.; Krishnan, V.; Monnier, A.; Grätzel, M. *J. Phys. Chem.* **1987**, *91*, 2342.
(12) Schaafsma, T. J. *Sol. Energy Mater. Sol. Cells* **1995**, *38*, 349.
(13) Boschloo, G. K.; Goossens, A. *J. Phys. Chem.* **1996**, *100*, 19489.
(14) Otero, L.; Osora, H.; Li, W.; Fox, M. A. *J. Porphyrins Phthalocyanines* **1998**, 2, 123.
(15) Mao, H.; Deng, H.; Li, P. H.; Shen, Y.; Lu, Z.; Xu, H. *J. Photochem. Photobiol., A* **1998**, *114*, 209.
(16) Yanagi, H.; Chen, S.; Lee, P. A.; Nebesny, K. W.; Armstrong, N.; Fujishima, A. *J. Phys. Chem.* **1996**, *100*, 5447.
(17) Kajihara, K.; Tanaka, K.; Hirao, K.; Soga, N. *Jpn. J. Appl. Phys.* **1998**, *35*, 6110.
(18) Fang, J.; Wu, J.; Lu, X.; Shen, Y.; Lu Z. *Chem. Phys. Lett.* **1997**, *270*, 145.
(19) Deng, H.; Mao, H.; Lu, Z.; Xu, H. *Thin Solid Films* **1998**, *315*, 244.
(20) Deng, H.; Lu, Mao, H.; Z.; Xu, H. *Chem. Phys.* **1997**, *221*, 323.
(21) Deng, H.; Lu, Mao, H.; Z.; Shen, Y. *J. Chem. Soc., Faraday Trans.* **1998**, *94*, 659.
(22) Deng, H.; Lu, Shen, Y. Mao, H.; Z.; Xu, H. *Chem. Phys.* **1998**, *231*, 95.
(23) Kampas, F. J.; Yamashita, K.; Fajer, J. *Nature* **1980**, *284*, 40.
(24) Harima, Y.; Yammamoto, K.; Takeda, K.; Yamashita, K. *Bull. Chem. Soc. Jpn.* **1989**, *62*, 1458.
(25) Gregg, B. A.; Fox, M. A.; Bard, A. J. *J. Phys. Chem.* **1990**, *94*, 1586.
(26) Antohe, S. *Phys. Status Solidi (a)* **1993**, *136*, 401.
(27) Takahashi, K.; Nanbu, H.; Komura, T.; Murata, K. *Chem. Lett.* **1993**, 613.
(28) Takahashi, K.; Hashimoto, K.; Komura, T.; Murata, K. *Chem. Lett.* **1994**, 269.
(29) Fox, M. A.; Grant, J. V.; Melamed, D.; Torimoto, T.; Liu, C.-Y.; Bard, A. J. *Chem. Mater.* **1998**, *10*, 1771.
(30) Tennakone, K.; Kumara, G. R. R. A.; Kumarasinghe, A. R.; Wijayantha, K. G. U.; Sirimanne, P. M. *Semicond. Sci. Technol.* **1995**, *10*, 1689.
(31) O'Regan, B.; Schwartz, D. T. *J. Appl. Phys.* **1996**, *80*, 4749.
(32) Tennakone, K.; Kumara, G. R. R. A.; Wijayantha, K. G. U.; Kottegoda, I. R. M.; Perera, V. P. S.; Aponsu, G. M. L. P. *J. Photochem. Photobiol., A* **1997**, *108*, 175.
(33) Hagen, J.; Schaffrath, W.; Otschik, P.; Fink, R.; Bacher, A.; Schmidt, H.-W.; Haarer, D. *Synth. Met.* **1997**, *89*, 215.
(34) Tennakone, K.; Kumara, G. R. R. A.; Kottegoda, I. R. M.; Wijayantha, K. G. U.; Perera, V. P. S. *J. Phys. D: Appl. Phys.* **1998**, *31*, 1492.
(35) Salafsky, J. S.; Lubberhuizen, W. H.; Schropp, R. E. I. *Chem. Phys. Lett.* **1998**, *290*, 297.
(36) Fernando, C. A. N. *Sol. Energy Mater. Sol. Cells* **1992**, *28*, 255.
(37) Fernando, C. A. N. *Sol. Energy Mater. Sol. Cells* **1993**, *30*, 211.
(38) Isoda, S.; Nishikawa, S.; Ueyama, S.; Hanazato, Y.; Kawakubo, H.; Maeda, M. *Thin Solid Films* **1992**, *210*, 290.
(39) Gunster, S.; Siebentritt, S.; Meissner, D. *Mol. Cryst. Liq. Cryst.* **1993**, *230*, 351.
(40) Karl, N.; Bauer, A.; Holzäpfel, J.; Marktanner, J.; Möbus, M.; Stölzle, F. *Mol. Cryst. Liq. Cryst.* **1994**, *252*, 243.
(41) Wöhrle, D.; Kreienhoop, L.; Schnurpfeil, G.; Elbe, J.; Tennigkeit, B.; Hiller, S.; Schlettwein, D. *J. Mater. Chem.* **1995**, *5*, 1819.

(42) Savenije, T. J.; Koehorst, R. B. M.; Schaafsma, T. J. *Chem. Phys. Lett.* **1995**, *244*, 363.
(43) Savenije, T. J.; Moons, E.; Boschloo, G. K.; Goossens, A.; Schaafsma, T. J. *Phys. Rev. B* **1997**, *55*, 9685.
(44) Takahashi, K.; Nakatani, S.; Yamaguchi, T.; Komura, T.; Ito, S.; Murata, K. *Sol. Energy Mater. Sol. Cells* **1997**, *45*, 127.
(45) Kerp, H. R.; Donker, H.; Koehorst, R. B. M.; Schaafsma, T. J.; van Faassen, E. E. *Chem. Phys. Lett.* **1998**, *298*, 302.
(46) Signerski, R.; Jarosz, G.; Godlewski, J. *Synth. Met.* **1998**, *94*, 135.
(47) Bignozzi, C. A.; Argazzi, R.; Schoonover, J. R.; Meyer, G. J.; Scandola, F. *Sol. Energy Mater. Sol. Cells* **1995**, *38*, 187.
(48) He, J.; Zhao, J.; Shen, T.; Hidaka, H.; Serpone, N. *J. Phys. Chem. B* **1997**, *101*, 9027.
(49) Anton, J. A.; Loach, P. A.; Govindjee. *Photochem. Photobiol.* **1978**, *28*, 235.
(50) Brookfield, R. L.; Ellul, H.; Harriman, A.; Porter, G. *J. Chem. Soc., Faraday Trans.* **1986**, *82*, 219.
(51) Wienke, J.; Kleima, F. J.; Koehorst, R. B. M.; Schaafsma, T. J. *Thin Solid Films* **1996**, *279*, 87.
(52) Adler, A. D.; Longo, F. R.; Kampas, F.; Kim, J. *J. Inorg. Nucl. Chem.* **1970**, *32*, 2443.
(53) Little, R. G.; Anton, J. A.; Loach, P. A.; Ibers, J. A. *J. Heterocycl. Chem.* **1975**, *12*, 343.
(54) Little, R. G. *J. Heterocycl. Chem.* **1978**, *15*, 203.
(55) Wienke, J.; Kroon, J. M.; Sommeling, P. M.; Kinderman, R.; Späth, M.; van Roosmalen, J. A. M.; Sinke, W. C.; Baumgärtner, S. *Proc. 14th Eur. Photovoltaic Sol. Energy Conf., Barcelona.* **1997**, *06/30-07/04*, 1808.
(56) Weller, Z. Z. *Phys. Chem.* **1982**, *133*, 93.
(57) Hofstra, U.; Koehorst, R. B. M.; Schaafsma, T. J. *Chem. Phys. Lett.* **1986**, *130*, 555.
(58) Gaines, G. L.; O'Neil, M. P.; Svec, W. A.; Niemczyk, M. P.; Wasielewski, M. R. *J. Am. Chem. Soc.* **1991**, *113*, 719.
(59) Wienke, J.; Goossens, A.; Schaafsma, T. J. *J. Phys. Chem. B.* **1999**, *103*, 2702.
(60) Koehorst, R. B. M.; Maas, H.; Schaafsma, T. J., manuscript in preparation.
(61) Förster, Th. *Ann. Phys.* **1948**, *2*, 55.